which gave the approximate relationship $\delta(\Delta_1 r) = -9\delta l$. None of the refined values of the other parameters in Tables I and II were found to be very sensitive to the remaining assumptions. The bracketed values for the three difference parameters in Table I were obtained from molecular-mechanics calculations and that for C=C—H is similar to values in other molecules. Small changes in any of these quantities should not significantly affect the refinement results.

The two sets of results in Table I are in pleasing agreement and are each fair statements of the COD structure. We choose the set based on the OSU data as our preferred model because of the way in which the backgrounds were removed to generate the molecular intensities on which the refinements were based: the computer-generated backgrounds used with the OSU data are presumably less subject to bias than are the hand-drawn backgrounds used with the Oslo data. Table II is a more complete set of distances and amplitudes for the preferred model, and Table III is an abbreviated correlation matrix.

Discussion

As may be seen from Table IV, our structure for COD agrees well with the results of molecular-mechanics calculations, particularly those of Ermer[7] and Anet and Kozerski.[18] Table IV also shows that the conformation of the COD ring is not affected by the presence of pseudoequatorial substituents: the ring parameters of the two COD derivatives have values very similar to those for COD itself.

The carbon–carbon bond lengths in COD are quite similar to those found in aliphatic chains and in other low-strain ring systems. They require no special comment. The two types of bond angles (those adjacent and those not adjacent to the double bonds) are a few degrees larger than their open-chain counterparts, presumably mostly as a consequence of cross-ring repulsions which tend to flatten the carbon skeleton. The twisted-boat conformation adopted by the molecule is also consistent with an important role for repulsive interactions. For example, in both the chair and symmetric-boat forms vicinally situated pairs of carbon atoms are eclipsed, as are pairs of hydrogen atoms on adjacent methylene groups. The strains arising from these energetically unfavorable geometries are partially relieved in the twisted boat. Quantitative evidence for this qualitative picture is available from the molecular-mechanics calculations,[7,8] especially those of Ermer where the individual components of the potential are tabulated for several conformations of the molecule. The twisted-boat form was found to be lower in potential energy than the regular boat by 7 kcal/mol and the chair by 4 kcal/mol. The calculations are also consistent with our conclusion that large-amplitude torsional vibration is not present in COD, a crude estimate based upon the potential-energy profiles for twisting suggesting that more than 85% of the molecules are to be found within 15° of the equilibrium values of $\angle C_3—C_4—C_5=C_6$ and $\angle C_2—C_3—C_4—C_5$.

Our final remarks concern the possible presence of other conformers in our gaseous samples. Although our tests for the chair form were negative, they can only be interpreted as ruling out substantial amounts of that form. When small amounts of chair were included in composition-constrained calculations, the structural results and agreement with experiment did not differ significantly from those obtained with the twisted boat as the only form present. From these calculations we estimate that more than about 10% of the chair in our samples would be incompatible with the electron-diffraction data but that smaller amounts cannot be excluded. Although forms other than the chair were not tested, the same statements may be assumed to apply to them. These conclusions are consistent with the free energies of formation calculated from molecular mechanics which, for example, in the case of the chair and twisted-boat forms, corresponds to only about 1% of the former in an equilibrium mixture.

Acknowledgment. We are grateful to the National Science Foundation for support of this work under Grant CHE-78-04258. K. Hagen thanks the Norges Almenvitenskapelige Forsknigsråd for a travel grant and partial support. K. Hedberg is indebted to the same organization for a stipend during which the Oslo work was carried out.

Supplementary Material Available: Tables of the leveled total intensities (Table V), calculated backgrounds (Table VI), average curves from each camera distance (Table VII), symmetry coordinates (Table VIII), and observed and calculated wave numbers (Table IX) (23 pages). Ordering information is found on any current masthead page.

(18) Anet, F. A. L.; Kozerski, L., private communication.

Rate Constant and Possible Pressure Dependence of the Reaction OH + HO_2

W. B. DeMore

Jet Propulsion Laboratory, California Institute of Technology, Pasadena, California 91107 *(Received: July 7, 1981; In Final Form: September 2, 1981)*

The technique of laser-induced fluorescence has been used to measure steady-state OH concentrations in the photolysis of water vapor at 184.9 nm and 298 K, with O_2 added in trace amounts. He or Ar was present at total pressures in the range 75–730 torr. The results were used to derive the rate-constant ratio $k_1/k_5^{1/2}$, where k_1 and k_5 are the rate constants for the reactions $OH + HO_2 \rightarrow H_2O + O_2$ and $HO_2 + HO_2 \rightarrow O_2$, respectively. When currently available values for k_5 are used, the results give $k_1 = (1.2 \pm 0.4) \times 10^{-10}$ cm^3 s^{-1} at 1-atm pressure, with evidence of a decline of k_1 at lower pressures. No water-vapor effect on k_1 was observed.

Introduction

Reliable measurement of the rate constant for the reaction

$$OH + HO_2 \xrightarrow{k_1} H_2O + O_2 \quad (1)$$

has been a long-standing problem in kinetics.[1-4] The

0022-3654/82/2086-0121$01.25/0

difficulty in measuring this rate is related to several factors, such as the radical–radical nature of the reaction, the problem of monitoring the radical concentrations (especially HO_2), and the tendency of the reactants to undergo complicating side reactions or self-reactions. The situation is further complicated by the possibility that this reaction, usually assumed to be strictly bimolecular, may proceed by a complex mechanism involving an intermediate adduct such as H_2O_3.[2,5] This question is referred to later in the Discussion section dealing with possible pressure dependence of the reaction.

Earlier measurements of k_1 in low-pressure systems (i.e., a few torr) have fallen in the range of about 3×10^{-11} cm^3 s^{-1} (ref 6 and 7) to 5.1×10^{-11} cm^3 s^{-1} (ref 8). However, more recent results under these conditions by Keyser[9] have given the somewhat higher value of 6.5×10^{-11} cm^3 s^{-1}. By contrast, measurements near 1 atm[3,4,10-13] have consistently yielded k_1 values of $\geq 1 \times 10^{-10}$ cm^3 s^{-1}. This discrepancy has led to the suggestion[4] of a possible pressure dependence for the reaction. However, additional systematic studies of the possible pressure dependence are needed.

The present work has had two principal objectives: first, to obtain further measurements of k_1 at pressures near 1 atm, and, second, to examine the pressure dependence. The experiments involved steady-state photolysis of H_2O in the presence of a small amount of O_2, under which conditions $[OH]_{ss}$ is sensitive to k_1. The $[OH]_{ss}$ was measured by laser-induced fluorescence, which was calibrated on an absolute basis.

Experimental Methods

Mechanism. The basic photochemical mechanism used in these experiments can be given as follows:

$$H_2O \xrightarrow{184.9\ \text{nm}} H + OH \quad (2)$$

$$H + O_2 + M \rightarrow HO_2 + M \quad (3)$$

$$OH + HO_2 \rightarrow H_2O + O_2 \quad (1)$$

$$OH \rightarrow \text{products} \quad (4)$$

$$HO_2 + HO_2 \rightarrow H_2O_2 + O_2 \quad (5)$$

$$OH + H_2O_2 \rightarrow H_2O + HO_2 \quad (6)$$

Addition of H_2 in measured concentrations served to convert OH to HO_2, by reaction 7 followed by reaction 3.

$$OH + H_2 \rightarrow H_2O + H \quad (7)$$

This has the effect of changing the OH/HO_2 ratio, and introduces a variable but controllable first-order OH loss rate which can be made to dominate reaction 4.

The rate constant k_4 represents the effective first-order loss of OH by several possible paths, including reaction with trace impurities and diffusive loss to the walls. In the calibration procedure (described later), it was found that k_4 usually was in the range 3–5 s^{-1}. Radical–radical reactions (with HO_2 absent) are not fast enough to account for these rates under the conditions of the experiments, although the reactions

$$OH + OH + M \rightarrow H_2O_2 + M \quad (8)$$

$$OH + OH \rightarrow H_2O + O \quad (9)$$

could give loss rates approaching 1 s^{-1} at the highest OH concentrations used, about 10^{11} cm^{-3}. It is believed that k_4 was due mainly to reaction of OH with hydrogenous impurities in the reaction mixtures. Hydrocarbon impurities of a few tenths of a ppm would be adequate, assuming a rate constant for reaction with OH of about 10^{-12} cm^3 s^{-1}. Diffusive loss was relatively unimportant, except possibly at the lowest pressures used. With added H_2, first-order loss of OH by reaction 7 dominated k_4 in many of the experiments, with no effect on the results. Thus, the precise nature of k_4 is not critical to the interpretation of the results.

To produce HO_2 in the mixtures, oxygen was added at pressures in the range of about 0.1–0.3 torr, which was found to be sufficient to convert all H into HO_2 by reaction 3. The effect of increasing conversion of H to HO_2 upon addition of O_2 could be seen by monitoring the OH signal as O_2 was added, showing a rapid fall in [OH] due to the appearance of HO_2. The [OH] eventually leveled off at a constant value when the scavenging of H was complete, and additional O_2 had no further effect. Because of the low O_2 cross section at 184.9 nm compared to that of H_2O (factor of 7),[3] these small O_2 pressures did not affect the OH concentration by the processes

$$O_2 + 184.9\ \text{nm} \rightarrow O + O \quad (10)$$

$$O + OH \rightarrow O_2 + H \quad (11)$$

$$O + HO_2 \rightarrow OH + O_2 \quad (12)$$

Further, the O_2 quenching rate for OH fluorescence is not large enough compared to that of H_2O to affect the fluorescence efficiency,[14,15] as was verified in the present work.

Both experiment and computer simulation (discussed later) showed that reaction 6 can be neglected on the time scale over which the $[OH]_{ss}$ measurements were made, which was about 5 s after onset of photolysis. This is because of the relatively slow rate of H_2O_2 formation in the mixture, combined with the known rate constant[16,17] for reaction 6 which is considerably slower than the rate constant for reaction of OH with HO_2.

Steady-state considerations show that

$$(k_4 + 2k_7[H_2])[OH]_{ss} = 2k_5[HO_2]_{ss}^2 \quad (13)$$

because loss of OH by reaction 4 and 7 must be balanced by loss of HO_2 through reaction 5.

Additionally, the steady-state OH concentration is given by

$$[OH]_{ss} = I_a^{H_2O}/(k_4 + k_1[HO_2]_{ss} + k_7[H_2]) \quad (14)$$

where $I_a^{H_2O}$ is the rate of H_2O photolysis.

(1) F. Kaufman in "Atmospheres of Earth and the Planets", B. M. McCormac, Ed., Dordrecht, Holland, 1975, p 219; *Annu. Rev. Phys. Chem.*, **30**, 411 (1977).
(2) C. J. Howard in "Proceedings of the NATO Advanced Study Institute on Atmospheric Ozone: Its Variation and Human Influences", M. Nicolet, Director, A. A. Aikin, Ed., U.S. Department of Transportation, 1979, Report No. FAA-EE-80-20, p 409.
(3) W. B. DeMore and E. Tschuikow-Roux, *J. Phys. Chem.*, **78**, 1447 (1974).
(4) W. B. DeMore, *J. Phys. Chem.*, **83**, 1113 (1979).
(5) J. P. Burrows, R. A. Cox, and R. G. Derwent, *J. Photochem.*, **16**, 147 (1981).
(6) J. S. Chang and F. Kaufman, *J. Phys. Chem.*, **82**, 1683 (1978).
(7) W. Hack, A. W. Preuss, and H. Gg. Wagner, *Ber. Bunsenges. Phys. Chem.*, **82**, 1167 (1978).
(8) J. P. Burrows, G. W. Harris, B. A. Thrush, *Proc. R. Soc. London, Ser. A*, **368**, 463 (1979).
(9) L. F. Keyser, *J. Phys. Chem.*, in press.
(10) C. J. Hochanadel, T. J. Sworski, and P. J. Ogren, *J. Phys. Chem.*, **84**, 3274 (1980).
(11) C. J. Hochanadel, J. A. Ghormley, and P. J. Ogren, *J. Chem. Phys.*, **56**, 4426 (1972).
(12) R. R. Lii, R. A. Gorse, Jr., M. C. Sauer, Jr., and S. Gordon, *J. Phys. Chem.*, **84**, 819 (1980).
(13) R. A. Cox, J. P. Burrows, and T. J. Wallington, to be submitted for publication.
(14) K. R. German, *J. Chem. Phys.*, **64**, 4065 (1976).
(15) P. M. Selzer and C. H. Wang, *J. Chem. Phys.*, **71**, 3786 (1979).
(16) L. F. Keyser, *J. Phys. Chem.*, **84**, 1659 (1980).
(17) U. C. Sridharan, B. Reimann, and F. Kaufman, *J. Chem. Phys.*, **73**, 1280 (1980).

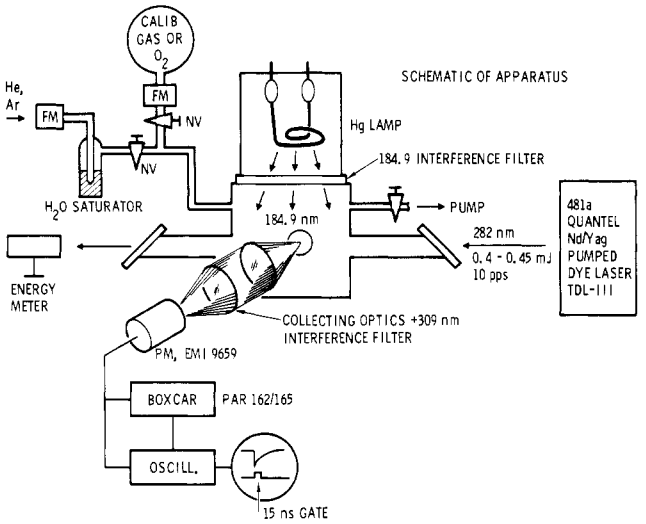

Figure 1. Schematic of apparatus.

Combination of eq 13 and 14 yields the following relationship between the measured steady-state OH concentrations and the rate constants k_1 and k_5:

$$\frac{k_1}{k_5^{1/2}} = \frac{I_a^{H_2O} - (k_4 + k_7[H_2])[OH]_{ss}}{[OH]_{ss}^{3/2}\left[\frac{k_4 + 2k_7[H_2]}{2}\right]^{1/2}} \quad (15)$$

In the application of eq 15, $[H_2]$ was varied, but conditions were always chosen such that $I_a^{H_2O} \gg k_7[H_2][OH]_{ss}$. This was to ensure that most of the OH reacted with HO_2 rather than with H_2, which thereby retained a high sensitivity of $[OH]_{ss}$ to k_1. This condition was possible because k_4 was small.

$I_a^{H_2O}$ was calculated from the expression

$$I_a^{H_2O} = I_0\sigma_{H_2O}n_{H_2O} \quad (16)$$

where I_0 is the 184.9-nm intensity (quanta cm^{-2} s^{-1}), σ_{H_2O} is the cross section for H_2O at 184.9 nm (7.8×10^{-20} cm^2),[3] and n_{H_2O} is the H_2O concentration in particles cm^{-3}. The quantity I_0 was determined actinometrically by measuring the rate of O_2 photolysis to produce O_3 in small quartz cells which were placed inside the fluorescence cell. Corrections for window absorption were made on the basis of measured absorbances of the empty cells and the assumption of equal absorbances by the front and back windows. The resulting corrections were in the range of 15–20%. Results in cells of path lengths 1 and 5 cm were identical to within 5%, suggesting reasonable uniformity of light intensity. Thus

$$I_a^{O_2} = \frac{1}{2}\frac{\Delta[O_3]}{\Delta t} = I_0\sigma_{O_2}n_{O_2} \quad (17)$$

where $\sigma_{O_2} = 1.08 \times 10^{-20}$ cm^2.[3] The actual absorbed light intensities were in the range 1×10^{11}–7×10^{11} quanta cm^{-2} s^{-1}, depending on the H_2O pressure used. It should be pointed out that the results are sensitive only to approximately the square root of $I_a^{H_2O}$, because the quantity $[OH]_{ss}$ in eq 15 is proportional to $I_a^{H_2O}$.

Apparatus. A schematic diagram of the apparatus is shown in Figure 1. The carrier gases He or Ar were passed through an H_2O bubbler which was temperature controlled in order to establish the desired H_2O pressure. The carrier gases were HP or GC grades and, in some cases, were first passed through a Matheson Hydrox purifier to remove traces of O_2, followed by a molecular sieve trap at −78 or −196 °C to minimize other impurities. Total pressure ranged from 75 to 730 torr, with water pressures of 1–5 torr. Flow rates were varied but usually were near 300 sccm, corresponding to cell flushing times of 1–2 min. Flow rates were measured by means of calibrated flowmeters (Hastings-Teledyne), and cell pressures were monitored with a calibrated Baratron gauge. The photolysis source was a low-pressure mercury lamp, combined with a 184.9-nm interference filter to limit radiation to that wavelength. Gases such as O_2 or the calibrating gases H_2 and CH_4 were added to the flowing stream from bulb reservoirs. Two fluorescence cells were used; one was of stainless steel coated on the inside with Teflon, and the other was of uncoated Pyrex. Each cell had Suprasil quartz windows for the laser beam and for the fluorescence signal. The object of using two cell types was to test for possible surface effects. The cells were approximately cylindrical, with diameter 10 cm and depth 10 cm.

The laser-induced fluorescence system was similar to that previously described by Davis and co-workers.[18] The fluorescence excitation source was a dye laser (Quantel TDL-111) pumped by a Quantel 481a Nd:YAG laser. The system was operated at 10 pulses s^{-1} with an average pulse energy of 0.425 ± 0.025 mJ $pulse^{-1}$. The pulse width was 7 ns. Pulse energies were monitored with a Laser Precision Corp. meter, type Rj-7100. The laser beam width was approximately 2 mm.

To minimize background signal arising from source scatter, the $Q_1(1)$ line near 281.9 nm in the $^2\pi(v'' = 0) \rightarrow {}^2\Sigma(v' = 1)$ system was excited and nonresonant emission near 309 nm ($v'' = 0 \rightarrow v' = 0$) was observed. As illustrated in Figure 1, an optical collection system consisting of two 5-cm focal length quartz lenses was used to focus an image of the fluorescence beam onto the face of the photomultiplier tube (EMI 9659). A slit on the face of the photomultiplier tube limited the transmitted radiation to that of the beam image. An interference filter with transmission centered at 309 nm was used to minimize background fluorescence. The photomultiplier output was observed with a Tektronix 475 oscilloscope, and the intensity was measured with a PAR 162 boxcar analyzer, equipped with the Model 165 integrator module. A gate width of 15 ns was used.

The background fluorescence signal with zero OH concentration was about 1% of the maximum signal obtained for $[OH] \sim 10^{11}$ cm^{-3}. The background signal was found to vary somewhat, depending mainly on how long the photolytic lamp had been on. This is believed to be due to cleaning up of wall contaminants (by OH) which fluoresce upon absorption of scattered laser light.

Results

Calibration of the Fluorescence Signal. Absolute OH concentrations were determined by use of a calibration factor relating concentration to fluorescence intensity

$$[OH] = \alpha(cm^{-3}\ mV^{-1}) \times S(mV) \quad (18)$$

where S was the observed boxcar signal in mV for a given OH concentration. A linear relationship between OH concentration and fluorescence signal was verified in the calibration procedure, which involved addition of known concentrations of the calibrating gas, G (usually CH_4 or H_2), to the photolysis of H_2O in pure carrier gas. Thus

$$[OH]_{ss}^{cal} = I_a^{H_2O}/(k_4 + k_G[G]) \quad (19)$$

where [G] is the concentration of calibrating gas and k_G is the rate constant for the reaction of OH with the gas G. Combined with eq 18, the following linear relationship

(18) D. D. Davis, W. S. Heaps, D. Philen, M. Rodgers, T. McGee, A. Nelson, and A. J. Moriarty, *Rev. Sci. Instrum.*, 50, 1505 (1979).

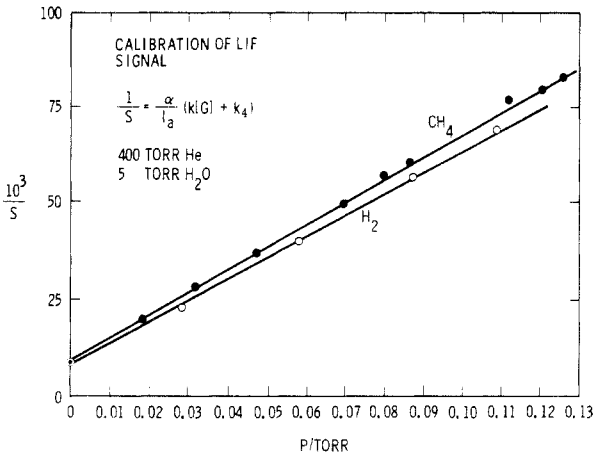

Figure 2. Example of calibration data.

is predicted for the reciprocal of the fluorescence intensity and [G]:

$$1/S = (\alpha/I_a^{H_2O})(k_G[G] + k_4) \quad (20)$$

Thus, a plot of $1/S$ vs. [G] yields α from the slope and k_4 from the intercept.

Figure 2 shows an example of calibration data for a mixture with 400 torr of He and 5 torr of H_2O, with added CH_4 and H_2. As predicted from eq 20, the reciprocal of the fluorescence signal was found to be linear with concentration (pressure) of the added gas. Furthermore, the ratio of slopes (0.91) was found to agree very well with recommended rate constants[19] for the reactions of OH with H_2 and CH_4, $k_{H_2} = 7.1 \times 10^{-15}$ cm^3 s^{-1} and $k_{CH_4} = 8.0 \times 10^{-15}$ cm^3 s^{-1}. A few experiments were also carried out with CO as the calibrating gas. The relative slope obtained with CO corresponded to the rate constant $k_{CO} = 1.5 \times 10^{-13}$ cm^3 s^{-1}, which is consistent with the recommended rate constant for this reaction at low pressure.[19] This result therefore agrees with the finding of Biermann et al.[20] that k_{CO} exhibits no pressure enhancement when O_2 is absent.

Rigorous exclusion of O_2 from the calibration mixtures was necessary in order to obtain accurate and consistent results for the various calibration gases. This was because the presence of O_2 impurity led to the partial conversion of H to HO_2, which then introduced a source of OH by the reaction

$$H + HO_2 \rightarrow OH + OH \quad (21)$$

For high ratios of H to OH, such as are obtained when only a trace amount of O_2 is present, and gases such as H_2 or CO have been added, reaction 21 dominates OH loss from reaction 1 and a net gain in OH is realized. The effect of reaction 21 was seen clearly in H_2 and CO calibration experiments in which O_2 was present as an impurity at the ppm level. Under these circumstances the calibration plots were nonlinear and did not show the correct relative slopes with respect to CH_4. The O_2 effect was demonstrated experimentally as follows. In the presence of sufficient added H_2 to reduce the OH signal by a factor of about 8, deliberate addition of O_2 at 5 ppm caused a threefold increase in the OH signal. In contrast to H_2 and CO, CH_4 did not show a high sensitivity to O_2 contamination, since reaction of OH with CH_4 does not produce H, as is the case with both H_2 and CO. Other factors may be involved, such as the scavenging of O_2 by CH_3 radicals. In general, CH_4 was found to be preferable as the calibrating gas, largely for this reason.

TABLE I: Summary of Results for $k_1/k_5^{1/2}$

press., torr	[H_2O], torr	carrier gas	$10^5 k_1/k_5^{1/2}$, cm$^{3/2}$ s$^{-1/2}$ metal cell no H_2	metal cell H_2	glass cell no H_2	glass cell H_2	av
730	5	Ar				6.2	6.2
400	5	He	6.1	5.2	6.9	5.6	6.0
400	5	Ar	6.8	5.2			6.0
200	2.5	He	5.2	4.0	5.1	4.0	4.6
200	2.5	Ar	6.3	5.0		5.0	5.4
75	0.94	He	4.6	4.0			4.3
75	0.94	Ar	5.8	5.8			5.8
75	4.6	He	4.0	4.6			4.3
75	4.6	Ar	5.2	4.6			4.9

The calibration factors depended mainly on the H_2O concentration and not on the pressure of carrier gas, because H_2O dominated the quenching efficiency of the mixtures. Calibration factors were measured immediately before each experiment, although the results were usually quite reproducible from one experiment to the next.

The quantity k_4 was in the range of about 9–10 s^{-1} in the earliest experiments in the metal cell but subsequently declined to about 3–5 s^{-1}. This change with time is believed to have resulted from gradual removal of hydrogenous contaminants from the apparatus. The glass cell, which was introduced at a later stage of the experiments, did not show the initially high k_4 values.

The approximate correctness of k_4 as measured in the calibration procedure was verified by following the time decay of the OH fluorescence upon turning off the 184.9-nm lamp source. For this purpose a recording oscilloscope was used to follow several successive fluorescence traces (0.1-s intervals), which were triggered to coincide with each laser pulse. Although the accuracy of this approach was limited because of variation in laser-pulse power (roughly 25% pulse-to-pulse), the observed decay was in good agreement with the calibration values.

Steady-State Measurements of [OH]. Photolysis of pure water vapor in the carrier gas gave OH concentrations of the order of 10^{11} cm^{-3}, with the exact value depending on the water-vapor concentration. Upon addition of O_2, the OH concentration fell to the range $1 \times 10^{10} - 3 \times 10^{10}$ and declined further as H_2 was added. The OH reached (quasi-) steady state within about 1 s after opening of the photolysis lamp shutter. To avoid significant OH loss due to buildup of H_2O_2, we made the measurements within about 5–10 s. Because of the slow rate of H_2O_2 formation, the actual rate of change in [OH] was quite small. Some decrease with time was observed, as expected.

Table I shows a summary of results for the ratio $k_1/k_5^{1/2}$ obtained under various conditions of total pressure, mixture composition, and cell type. Each entry for added H_2 represents the average of about four separate measurements for different H_2 concentrations, all of which were sufficiently high to dominate the effect of k_4. No trend in the results with H_2 concentration was observed, although the results with no H_2 (k_4 important) were on the average slightly higher than those obtained with added H_2. Essentially identical values were obtained in the Teflon-coated cell and in the Pyrex cell, thus tending to argue against any role of surface effects or surface impurities. At lower pressures, the results obtained in Ar were slightly higher than in He. Individual values for the ratio $k_1/k_5^{1/2}$

(19) D. L. Baulch, R. A. Cox, R. F. Hampson, Jr., J. A. Kerr, J. Troe, and R. T. Watson, *J. Phys. Chem. Ref. Data*, **9**, 295–471 (1980).
(20) H. W. Biermann, C. Zetsch, and F. Stuhl, *Ber. Bunsenges. Phys. Chem.*, **82**, 633 (1978).
(21) "Chemical Kinetics and Photochemical Data for Use in Atmospheric Modelling", Evaluation No. 4, NASA Panel for Data Evaluation, Jet Propulsion Laboratory Publication 81-3, Jet Propulsion Laboratory, California Institute of Technology, Pasadena, CA.

TABLE II: Results for k_1

press., torr	$[H_2O]$, torr	carrier gas	$10^{12}k_5$,[a] $cm^3\ s^{-1}$	k_1, $cm^3\ s^{-1}$
730	5	Ar	3.8	1.2×10^{-10}
400	5	He	2.7	1.0×10^{-10}
400	5	Ar	3.2	1.1×10^{-10}
200	2.5	He	2.1	6.7×10^{-11}
200	2.5	Ar	2.4	8.4×10^{-11}
75	0.94	He	1.8	5.8×10^{-11}
75	0.94	Ar	1.9	8.0×10^{-11}
75	4.6	He	2.4	6.7×10^{-11}
75	4.6	Ar	2.6	7.9×10^{-11}

[a] Based on measurements of k_5 in He and Ar by S. P. Sander et al. (to be submitted for publication) combined with an enhancement of k_5 by water vapor as reported by Hamilton and Lii.[23]

for a series of measurements with different H_2 concentrations varied randomly by about 20%. The major source of variation is believed to have been the zero correction of the boxcar reading, which included both the background fluorescence level (about 10% of signal) and the zero setting of the boxcar, which drifted slightly.

To obtain absolute values of k_1, it is necessary to estimate the rate constant k_5 for the particular conditions of pressure and mixture composition used. There is currently some question about the exact pressure dependence of k_5. The values for the present comparison, shown in Table II, are based on recent measurements by Sander et al.,[22] combined with an additional factor to account for the water-vapor effect as reported by Hamilton and Lii.[23]

The $[HO_2]_{ss}$ concentrations as calculated from eq 13 were usually about 1 order of magnitude greater than $[OH]_{ss}$, and for different H_2 concentrations the ratio $[HO_2]/[OH]$ varied by a factor of about 5. As mentioned above, $k_1/k_5^{1/2}$ was independent of this variation, which tends to support the validity of the results.

Computer Simulations. Computer simulations of a typical reaction mixture were conducted on the basis of the reaction set 1–7. The purposes were to examine the steady-state behavior of OH and to assess the role of H_2O_2 as a loss path for OH. Literature values[19,21] were used for all reaction rate contants except for k_4 and k_1. For k_4 an experimental value of 4 s^{-1} was used, and k_1 was varied from 6×10^{-11} to 1.2×10^{-10} $cm^3\ s^{-1}$. The results showed that OH reached its (quasi-) steady-state value within about 1 s following onset of irradiation, in agreement with the experimental observation. The HO_2 also reached steady state in about 1 s. In the time period in which the OH steady-state measurements were made, H_2O_2 accounted for only about a 5% loss of OH, thus confirming the validity of neglecting reaction 6 for the derivation of eq 16.

Discussion

Magnitude of k_1. At pressures near 1 atm, the calculated value of k_1 is 1.2×10^{-10} $cm^3\ s^{-1}$, with an estimated uncertainty of ±30%. The major sources of error are believed to be the calculation of $[HO_2]_{ss}$ (which involves the reference rate constant k_5), possible errors in the rate constants for the calibration gases, small mechanistic effects such as the neglect of H_2O_2, and random errors involved in the background fluorescence signal.

The above value of k_1 is in excellent agreement with our previous measurement for 1 atm of an N_2/O_2 mixture, using a different technique.[3,4] The best values from the previous work were 1.2×10^{-10}–1.3×10^{-10} $cm^3\ s^{-1}$. The present result is also in good agreement with other recent measurements near 1 atm,[11-13] which give k_1 of about 1×10^{-10} $cm^3\ s^{-1}$.

Other than HO_2, there is no known species which can be produced in the present reaction mixtures upon addition of O_2 which can account for the observed OH loss rates. If such species were present before O_2 addition, the effect would be detected in the measurement of k_4. Production of hypothetical oxidized species which might be more reactive to OH than their precursors cannot take place on the time scale at which the measurements were made. Thus, there appears to be no reason to doubt that the observed OH loss was in fact due to reaction 1.

Pressure Dependence of k_1. Table II shows a downward trend of k_1 with decreasing pressure. These observations alone cannot be accepted as proof of a pressure dependence of k_1, because the effect is not clearly outside the experimental uncertainty. It is noteworthy, nevertheless, that the low-pressure results seem to be approaching the k_1 value obtained by Keyser[9] at a few torr, which was 6.5×10^{-11} $cm^3\ s^{-1}$. This comparison lends increasing support to the hypothesis of a pressure-dependent component of the reaction.

The decrease of k_1 with pressure is evidently not due to decreasing H_2O pressure. To test for this possibility, experiments at 75-torr total pressure were conducted with the H_2O partial pressure raised to nearly the same level as in the experiments at 730 torr. As seen in Table II, the result for k_1 was unchanged.

If the pressure dependence is real, the reaction mechanism must be more complex than that of a simple bimolecular abstraction. The abstraction reaction would involve a transition state of the form $(HO{\cdot}{\cdot}HO_2)^*$ but no long-lived intermediate.

$$OH + HO_2 \rightarrow (HO{\cdot}{\cdot}HO_2)^* \rightarrow H_2O + O_2 \qquad (22)$$

The reaction occurring by this mechanism cannot exhibit a pressure dependence. However, in addition to the abstraction path, the reaction can occur as a radical–radical association reaction, and the rate of product formation by this path can have both pressure-independent and pressure-dependent components. The mechanism of the pressure-independent component is as follows:

$$OH + HO_2 \rightleftarrows [H_2O_3]^* \qquad (23, -23)$$

$$[H_2O_3]^* \rightarrow H_2O + O_2 \qquad (24)$$

The effective rate constant is $k_{23}k_{24}/(k_{24} + k_{-23})$. This effective rate constant would be an additive term to the rate constant, k_{22}, for the abstraction reaction. Thus, the total low-pressure rate constant would be

$$k_1(\text{low pressure}) = k_{22} + k_{23}k_{24}/(k_{24} + k_{-23}) \qquad (25)$$

The fact that the observed value[9] for k_1 of 6.5×10^{-11} $cm^3\ s^{-1}$ is faster than expected for an abstraction reaction (not greater than about 1×10^{-11} $cm^3\ s^{-1}$) can be taken as support for the role of the radical–radical association component of the overall reaction.

At higher pressures the possibility of vibrational quenching of $[H_2O_3]^*$ gives rise to a pressure-dependent component of the reaction.

$$[H_2O_3]^* + M \rightarrow [H_2O_3] + M \qquad (26)$$

For the vibrationally relaxed (or perhaps partially relaxed) species H_2O_3, the rate-constant ratio $k_{24}^{relaxed}/k_{-23}^{relaxed}$ may be much higher than for $[H_2O_3]^*$, as would be the case if energy barrier for reaction −23 is greater than that for reaction 24. Thus, an apparent pressure enhancement

(22) S. P. Sander, M. Peterson, R. T. Watson, and R. Patrick, to be submitted for publication.
(23) E. J. Hamilton and R. R. Lii, *Int. J. Chem. Kinet.* 9, 875 (1977).

would be observed. In the limiting case where $k_{-23}^{relaxed}$ for H_2O_3 is effectively zero compared to $k_{24}^{relaxed}$, the overall expression for k_1 becomes

$$k_1 = k_{22} + k_{23}(k_{24} + k_{26}[M])/(k_{24} + k_{-23} + k_{26}[M]) \quad (27)$$

It is possible to indicate the broad ranges of parameters in eq 27 required for consistency with the observed rate-constant magnitude and apparent pressure enhancement. As previously mentioned, k_{22} is not expected to be greater than about 1×10^{-11} cm^3 s^{-1}, so that the quantity $k_{23}k_{24}/(k_{24} + k_{-23})$ must be at least 5×10^{-11} cm^3 s^{-1} to account for the total low-pressure observed k_1. To explain a pressure enhancement of k_1, one must place further constraints on the individual values of k_{23}, k_{24}, k_{-23}, and k_{26}. The data are well fitted by the values $k_{23} = 1.5 \times 10^{-10}$ cm^3 s^{-1}, $k_{24} = 1.5 \times 10^8$ s^{-1}, $k_{-23} = 3 \times 10^8$ s^{-1}, and $k_{26} = 2 \times 10^{-11}$ cm^3 s^{-1}. Small variations within this set of values would also fit the observations. The consistency of these rate constants with theoretical expectation is difficult to evaluate. The most critical unknown factor is the entropy of the intermediate $[H_2O_3]^*$, which determines the equilibrium constant k_{23}/k_{-23}. The high value of k_{23}/k_{-23} implied by the individual rate constants quoted above requires postulation of an extremely "loose" structure for $[H_2O_3]^*$.

Acknowledgment. This paper presents the results of one phase of research carried out at the Jet Propulsion Laboratory, California Institute of Technology, under Contract No. NAS7-100, sponsored by the National Aeronautics and Space Administration. I thank several members of the JPL Chemical Kinetics and Photochemistry Group for assistance with this work, including especially Drs. S. P. Sander, J. J. Margitan, R. T. Watson, M. Patapoff, and M. T. Leu. Very helpful advice on the resonance fluorescence method was provided by Dr. I. A. McDermid. Professor R. H. Smith, who was on study leave from MacQuarie University, New South Wales, Australia, aided in the development of the OH calibration procedure.

Electron Exchange between Tris(hexafluoroacetylacetonato)ruthenium(II) and -(III) and between Related Compounds. Effects of Solvent on the Rates[1]

Man-Sheung Chan and Arthur C. Wahl*

Department of Chemistry, Washington University, St. Louis, Missouri 63130 *(Received: August 11, 1981; In Final Form: September 21, 1981)*

The rate constants for electron exchange between $Ru(hfac)_3^-$ and $Ru(hfac)_3$, between $Ru(me_2bpy)(hfac)_2$ and $Ru(me_2bpy)(hfac)_2^+$, and between $Ru(me_2bpy)(acac)_2$ and $Ru(me_2bpy)(acac)_2^+$ have been measured by the NMR line-broadening method, hfac representing the hexafluoroacetylacetonate ion, acac representing the acetylacetonate ion, and me_2bpy representing 4,4′-dimethyl-2,2′-bipyridyl. The rate constants at 25 °C in acetonitrile are 5.0×10^6, 4.5×10^6, and 1.4×10^8 M^{-1} s^{-1}, respectively. The rate constants for the first two reactions vary with solvent dielectric properties about as predicted by the Marcus theoretical model; however, the preexponential coefficient, $\kappa\rho Z$, is 1 order of magnitude smaller than the value of $\sim 10^{11}$ M^{-1} s^{-1} generally assumed, possibly due to steric effects of the CF_3 groups. Measured temperature dependences of rate constants are small.

Introduction

The rates of electron exchange between $Ru(hfac)_3$ and $Ru(hafc)_3^-$, hfac representing the hexafluoroacetylacetonate ion, and between other neutral and singly charged complexes in various solvents are of interest because the main deterrent to electron transfer is probably the necessity for solvent reorganization.[2] There is no Coulombic repulsion between reactants, so the work required to bring them together is minimal, the standard free-energy change is zero for exchange reactions, and, for the exchange systems considered, the structures of the reactants are similar, so the energy required for internal rearrangement should be small and essentially the same for exchange in different solvents. Therefore, investigations of the rates of electron-exchange reactions in various solvents should increase our understanding of solvent-reorganizational requirements.

For exchange between ferrocene and ferrocenium ion, and also for several other systems, there is little dependence on solvent properties.[3] For several other systems, exchange rates do vary with solvent dielectric properties. These systems include those described in this article, $Ru(hfac)_3^{0,-}$ and $Ru(me_2bpy)(hfac)_2^{0,+}$, me_2bpy representing 4,4′-dimethyl-2,2′-bipyridyl, and the recently reported[4] exchange between $Cr(biph)_2^{0,+}$, biph representing biphenyl.

Experimental Section

$Ru(hfac)_3$ was purchased from Strem Chemicals, Inc., and it was purified by vacuum sublimation. Solutions of $Ru(hfac)_3^-$ salts in ethanol were prepared by reducing $Ru(hfac)_3$ with potassium iodide, tetramethylammonium iodide, or tetra-*n*-butylammonium iodide following the procedure by Patterson and Holm.[5] Solid products were obtained from the ethanolic solutions by addition of water. The salts $K[Ru(hfac)_3]$ and $Me_4N[Ru(hfac)_3]$ were purified by recrystallization from ethanol–water solutions. $Bu_4N[Ru(hfac)_3]$ was purified by reprecipitation from acetonitrile by addition of carbon tetrachloride. Analyses for carbon, hydrogen, and nitrogen, as well as analysis by spectrophotometric methods, indicated that these compounds were $> \sim 99\%$ pure.

$Ru(me_2bpy)(hfac)_2$ was synthesized from $Ru(me_2bpy)(H_2O)Cl_3$, which was prepared by the method

(1) Supported by the National Science Foundation under Grants CHE-76-02473 and CHE-80-03325.

(2) Marcus, R. A. *J. Chem. Phys.* **1965**, *43*, 679.

(3) Yang, E. S.; Chan, M.-S.; Wahl, A. C. *J. Phys. Chem.* **1980**, *84*, 3094.

(4) Li, T. T.-T.; Brubaker, C. H., Jr. *J. Organomet. Chem.* **1981**, *216*, 223.

(5) Patterson, G. S.; Holm, R. H. *Inorg. Chem.* **1972**, *11*, 2285.

0022-3654/82/2086-0126$01.25/0